

SPIN INJECTION INTO FERROMAGNETIC METAL FROM HEAVY METAL OWING TO SPIN HALL EFFECT

Yoshikazu Yamaki,¹ Syuta Honda,^{1*} and Hiroyoshi Itoh¹

(Received November 12, 2021)

Abstract

When a current flows through a heavy metal (HM), the spin of the current carriers is polarized by the spin Hall effect (SHE). In a junction of a HM and a ferromagnetic metal (FM), the spin current flows into the FM from the HM and gives spin-transfer torque to the magnetic moments of the FM. We calculate the spin current in a layer of HM/FM with the SHE. We use a spin-resolved electrochemical potential including the SHE in the calculation of the spin current. The spin current flowing into the FM depends strongly on the thickness of the HM.

1 Introduction

Spin injected into a ferromagnetic metal (FM) rotates the magnetic moments of the FM.^{1,2)} The spin injection reverses the magnetization of a nanosized FM³⁾ and drives a magnetic domain produced in a thin nanowire of FM.⁴⁾ A spin-orbit torque method is attracting attention as a method to apply torque to the magnetization of FM by spin injection.⁵⁾ In the structure of a heavy metal (HM) and FM multilayer, as shown in Fig. 1(a), the spin-orbit torque acts on magnetic moments in the FM. When a current flows through the HM, the spin of the current carriers is polarized by the spin Hall effect (SHE)^{6,7)} because the spin-orbit interaction of the HM is strong. The polarized spins are injected into the FM. A current of the polarized spin is called a spin current. The spin current flowing into the FM gives the spin-transfer torque the magnetic moments of the FM.^{1,2)} As a result, the magnetic moments in the FM take the torque owing to the spin-orbit interaction in the HM when the current flows through the HM. This is the spin-orbit torque.

In spintronics devices such as magnetoresistive random access memory (MRAM)⁸⁾ and racetrack memory⁹⁾, the magnetization of the FM is controlled. These high-speed spintronics devices require a fast magnetization reversal or a fast domain motion. The larger the spin-orbit torque is, the faster the domain moves.¹⁰⁾ In other words, the more spins are injected into the FM from the HM per unit time, the faster the domain moves. When the thickness of the HM is sufficiently longer than the spin diffusion length of the HM, the spin polarizes sufficiently. When the thickness of the FM is sufficiently longer than the spin diffusion length of the FM, the injected spin diffuses sufficiently in the FM. Both the spin diffusion lengths of

¹ Department of Pure and Applied Physics, Kansai University, Suita, Osaka 564-8680, Japan

* Correspondence to: Syuta Honda, Department of Pure and Applied Physics, Kansai University, Suita, Osaka 564-8680, Japan. E-mail: shonda@kansai-u.ac.jp

the HM and FM are a few nanometers.^{11),12)} However, the MRAM and the racetrack memory with the spin-orbit torque method are composed of a HM/FM layer with a few nanometers thickness. Hence both the spin polarization in the HM and the spin diffusion in the FM may be insufficient.

Designing devices using the spin-orbit torque requires clarification of the relation between the thickness of the HM/FM layer and the spin current flowing into the FM. We analyze the spin current flows into the FM from the HM in the HM/FM layer with a few nanometers thickness using a spin-resolved continuity equation of the carriers.

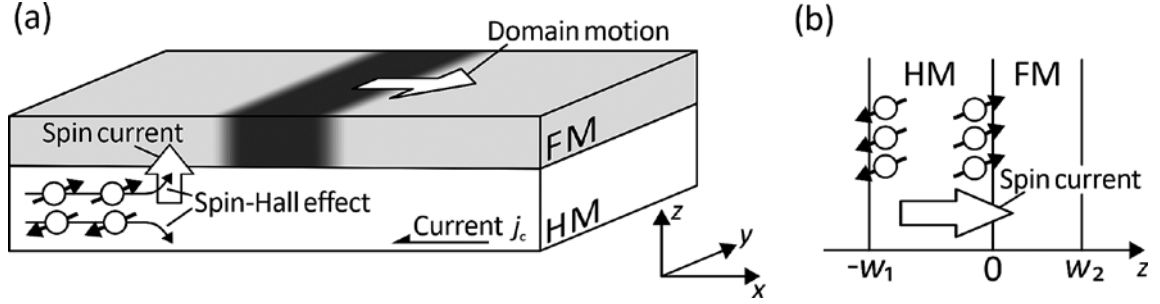


Fig. 1. Illustrations of (a) a domain motion due to a spin injection via a SHE of the HM layer in a HM/FM layer and (b) a one-dimensional model of the HM/FM layer with w_1 -thickness-HM and w_2 -thickness-FM.

2 Calculation results of the spin current

We focus on a HM/FM layer with finite thicknesses and infinite planes. An interface of the HM/FM layer is parallel to an x - y plane. In the HM with w_1 -thickness, a current is flowing along the $-x$ -direction. The spins of the $+y$ -direction are curved in the $+z$ -direction due to the SHE. The spins of the $-y$ -direction are curved in the $-z$ -direction due to the SHE. Hence, the spins are polarized. The FM with w_2 -thickness is set on the HM. Because not all variables depend on the x - or y -position, we use a one-dimensional model along the z -direction, as shown in Fig. 1(b).

A continuity equation of density of the spin-up of the carrier (n_{\uparrow}) is given as

$$\frac{dn_{\uparrow}}{dt} = -\frac{1}{q} \frac{dj_{\uparrow}}{dz} - \frac{n_{\uparrow}}{2\tau_{\uparrow 0}} + \frac{n_{\downarrow}}{2\tau_{\downarrow 0}} \quad (1)$$

and that of the spin-down of the carrier (n_{\downarrow}) is given as

$$\frac{dn_{\downarrow}}{dt} = -\frac{1}{q} \frac{dj_{\downarrow}}{dz} - \frac{n_{\downarrow}}{2\tau_{\downarrow 0}} + \frac{n_{\uparrow}}{2\tau_{\uparrow 0}}, \quad (2)$$

where t is time, q is the electron charge of -1.6×10^{-19} C, and $j_{\uparrow(\downarrow)}$ are the spin-resolved current densities of the spin-up (down) along the y -direction, $\tau_{\uparrow(\downarrow)0}$ are the spin relaxation times of spin-up (down). Here, the spin-up is pointing in the $+y$ -direction and the spin-down is pointing in the $-y$ -direction. $2\tau_{\uparrow(\downarrow)0}$ correspond to the time that the spin-up (down) state changes to the spin-down (up) state. For example, the second term of the right-hand side in Eq. (1) represents the amount by which the spin-up changes to spin-down per unit time. In a

paramagnetic metal such as a HM, the spin relaxation time is spin-independent ($\tau_{\uparrow 0} = \tau_{\downarrow 0}$). In contrast, the spin relaxation time usually depends on the spin in the FM ($\tau_{\uparrow 0} \neq \tau_{\downarrow 0}$). We assume that τ does not depend on the spin of FM ($\tau_{\uparrow 0} = \tau_{\downarrow 0} = \tau$).

The spin-resolved current densities $j_{\uparrow(\downarrow)}$ are given as

$$j_{\uparrow} = \sigma_{\uparrow} E_z - qD_{\uparrow} \frac{\partial n_{\uparrow}}{\partial z} - \theta_{\text{SH}} \frac{n_{\uparrow}}{n_{\uparrow} + n_{\downarrow}} j_c \quad (3)$$

and

$$j_{\downarrow} = \sigma_{\downarrow} E_z - qD_{\downarrow} \frac{\partial n_{\downarrow}}{\partial z} + \theta_{\text{SH}} \frac{n_{\downarrow}}{n_{\uparrow} + n_{\downarrow}} j_c, \quad (4)$$

where $\sigma_{\uparrow(\downarrow)}$ is the conductivity of each spin, E_z is an electric field along the z -direction, $D_{\uparrow(\downarrow)}$ is the diffusion coefficient of each spin, θ_{SH} is the spin Hall constant, and j_c is the density of the current along the $-x$ -direction. On the right-hand side of these equations, the first term is the density of the drift current, the second term is the density of the diffusion current, and the third term is the density of the spin-resolved current due to the SHE. Since the current flows along the $-x$ -direction, the spin current flows through along the z -direction due to the SHE. Because the current density j_c and the spin-resolved current due to the SHE do not depend on the x - or y -positions, $j_{\uparrow(\downarrow)}$ and $n_{\uparrow(\downarrow)}$ do not depend on the x - or y -positions. The electric field E_z occurs owing to the z -position-dependence of $n_{\uparrow} + n_{\downarrow}$ under the SHE but we do not estimate $n_{\uparrow} + n_{\downarrow}$. We assume that the conductivity $\sigma_{\uparrow(\downarrow)}$ and diffusion coefficient $D_{\uparrow(\downarrow)}$ are spin-independent ($\sigma_{\uparrow} = \sigma_{\downarrow} = \sigma$, $D_{\uparrow} = D_{\downarrow} = D$) and that the current density j_c does not depend on the z -position in the HM. Spin current density j_s is

$$j_s = \frac{\hbar}{2} \frac{1}{q} (j_{\uparrow} - j_{\downarrow}), \quad (5)$$

where $\hbar/2$ is the spin angular momentum and \hbar is the Dirac's constant. We define the difference of a spin-resolved electrochemical potential including the SHE $\delta\mu$ as

$$\delta\mu = k_B T \frac{n_{\uparrow}}{n_{\uparrow 0}} - k_B T \frac{n_{\downarrow}}{n_{\downarrow 0}} + \frac{q}{\sigma} \theta_{\text{SH}} j_c z, \quad (6)$$

where $n_{\uparrow(\downarrow)0}$ is the number of spin-up (down) of the carriers for a equilibrium state. By $\delta\mu$, $j_{\uparrow} - j_{\downarrow}$ for j_s is described as

$$j_{\uparrow} - j_{\downarrow} = -qD \frac{\partial(n_{\uparrow} - n_{\downarrow})}{\partial z} - \theta_{\text{SH}} j_c = -\frac{\sigma}{q} \frac{\partial \delta\mu}{\partial z}. \quad (7)$$

Here we used the Einstein relation, which relates the diffusion coefficient and electrical mobility μ_q , given as

$$D = \frac{\mu_q k_B T}{q} = \frac{\sigma k_B T}{q^2 n}, \quad (8)$$

where μ_q is electron mobility, k_B is the Boltzmann's constant, T is temperature, and n is the density of each carrier. Under the steady-state ($dn_{\uparrow(\downarrow)}/dt = 0$), a general solution of $\delta\mu$,

$$\delta\mu = A \exp\left(\frac{z}{\lambda}\right) + B \exp\left(-\frac{z}{\lambda}\right) + \frac{q}{\sigma} \theta_{\text{SH}} j_c z \quad (9)$$

is led, where A and B are arbitrary constants and λ is a spin diffusion length defined as $\lambda = (D\tau)^{1/2}$. Based on this general solution (9), we obtain the spin current density j_s in the HM/FM layer. In the HM ($-w_1 < z < 0$), the SHE occurs ($\theta_{\text{SH}} > 0, j_c > 0$), In the FM ($0 < z < w_2$), the SHE does not occur ($\theta_{\text{SH}} = 0$).

The general solution of $\delta\mu$ in the HM ($\delta\mu_{\text{HM}}$) becomes

$$\delta\mu_{\text{HM}} = A_{\text{HM}} \exp\left(\frac{z}{\lambda_{\text{HM}}}\right) + B_{\text{HM}} \exp\left(-\frac{z}{\lambda_{\text{HM}}}\right) + \frac{q}{\sigma_{\text{HM}}} \theta_{\text{SH}} j_c z \quad (10)$$

and the general solution of $\delta\mu$ in the FM ($\delta\mu_{\text{FM}}$) becomes

$$\delta\mu_{\text{FM}} = A_{\text{FM}} \exp\left(\frac{z}{\lambda_{\text{FM}}}\right) + B_{\text{FM}} \exp\left(-\frac{z}{\lambda_{\text{FM}}}\right). \quad (11)$$

If the spin scattering is neglected at both the interface and the surfaces, the boundary conditions are $j_{\text{sHM}}(-w_1) = 0, j_{\text{sHM}}(0) = j_{\text{sFM}}(0), j_{\text{sFM}}(w_2) = 0$, and $\delta\mu_{\text{HM}}(0) = \delta\mu_{\text{FM}}(0)$. Hence

$$A_{\text{HM}} = -\frac{\eta}{2\xi\sigma_{\text{HM}}} \left[\lambda_{\text{HM}}\sigma_{\text{FM}} \sinh\left(\frac{w_{\text{FM}}}{\lambda_{\text{FM}}}\right) + \lambda_{\text{FM}}\sigma_{\text{HM}} \left(\exp\left(\frac{w_{\text{HM}}}{\lambda_{\text{HM}}}\right) - 1 \right) \cosh\left(\frac{w_{\text{FM}}}{\lambda_{\text{FM}}}\right) \right], \quad (12)$$

$$B_{\text{HM}} = \frac{\eta}{2\xi\sigma_{\text{HM}}} \left[\lambda_{\text{HM}}\sigma_{\text{FM}} \sinh\left(\frac{w_{\text{FM}}}{\lambda_{\text{FM}}}\right) + \lambda_{\text{FM}}\sigma_{\text{HM}} \left(1 - \exp\left(-\frac{w_{\text{HM}}}{\lambda_{\text{HM}}}\right) \right) \cosh\left(\frac{w_{\text{FM}}}{\lambda_{\text{FM}}}\right) \right], \quad (13)$$

$$A_{\text{FM}} = -\frac{\eta}{\xi} \left[\lambda_{\text{FM}} \sinh^2\left(\frac{w_{\text{HM}}}{2\lambda_{\text{HM}}}\right) \exp\left(-\frac{w_{\text{FM}}}{\lambda_{\text{FM}}}\right) \right], \quad (14)$$

$$B_{\text{FM}} = -\frac{\eta}{\xi} \left[\lambda_{\text{FM}} \sinh^2\left(\frac{w_{\text{HM}}}{2\lambda_{\text{HM}}}\right) \exp\left(\frac{w_{\text{FM}}}{\lambda_{\text{FM}}}\right) \right] \quad (15)$$

are led. Here, η and ξ are given as

$$\eta = q\theta_{\text{SH}} j_c \lambda_{\text{HM}} \quad (16)$$

and

$$\xi = \lambda_{\text{HM}}\sigma_{\text{FM}} \cosh\left(\frac{w_{\text{HM}}}{\lambda_{\text{HM}}}\right) \sinh\left(\frac{w_{\text{FM}}}{\lambda_{\text{FM}}}\right) + \lambda_{\text{FM}}\sigma_{\text{HM}} \sinh\left(\frac{w_{\text{HM}}}{\lambda_{\text{HM}}}\right) \cosh\left(\frac{w_{\text{FM}}}{\lambda_{\text{FM}}}\right), \quad (17)$$

respectively.

The density of the spin current through the HM j_{sHM} and the FM j_{sFM} are led as

$$j_{\text{sHM}} = -\frac{\hbar}{2q} \frac{\sigma_{\text{HM}}}{q\lambda_{\text{HM}}} \left[A_{\text{HM}} \exp\left(\frac{z}{\lambda_{\text{HM}}}\right) - B_{\text{HM}} \exp\left(-\frac{z}{\lambda_{\text{HM}}}\right) \right] + \frac{\hbar}{2q} \theta_{\text{SH}} j_c \quad (18)$$

and

$$j_{s\text{FM}} = -\frac{\hbar}{2q} \frac{\sigma_{\text{FM}}}{q\lambda_{\text{FM}}} \left[A_{\text{FM}} \exp\left(\frac{z}{\lambda_{\text{FM}}}\right) - B_{\text{FM}} \exp\left(-\frac{z}{\lambda_{\text{FM}}}\right) \right], \quad (19)$$

respectively. Although the spin current is generated in the HM, the spin current depends on the spin diffusion length and the conductivity of the FM. The spin current in the FM decreases with increasing distance from the interface. The decay rate of the spin current in the FM depends on the spin diffusion length of FM.

In the cases of magnetization reversal and domain motion owing to the spin injection from the HM, the spin current density at the interface j_{s0} is important. The larger j_{s0} is, the larger the torque acting on the magnetic moments of the FM. From (19), the spin current density at the interface j_{s0} is led as

$$j_{s0} = \frac{\hbar}{2} \frac{\theta_{\text{SH}} j_c}{q\xi} \left[2\lambda_{\text{HM}} \sinh^2\left(\frac{w_{\text{HM}}}{2\lambda_{\text{HM}}}\right) \sinh\left(\frac{w_{\text{FM}}}{\lambda_{\text{FM}}}\right) \right]. \quad (20)$$

Under the limits of $w_{\text{HM}} \gg \lambda_{\text{HM}}$ and $w_{\text{FM}} \gg \lambda_{\text{FM}}$, j_{s0} becomes

$$j_{s0} = \frac{\hbar}{2} \frac{\lambda_{\text{HM}} \sigma_{\text{FM}}}{\lambda_{\text{HM}} \sigma_{\text{FM}} + \lambda_{\text{FM}} \sigma_{\text{HM}}} \frac{\theta_{\text{SH}} j_c}{q}. \quad (21)$$

The spin current density at the interface j_{s0} increases with the decreasing spin diffusion length of the FM λ_{FM} and increasing conductivity of the FM σ_{FM} . The j_{s0} is proportional to the current density j_c and the spin Hall angle θ_{SH} . When w_{HM} is equal to λ_{HM} and w_{FM} is equal to λ_{FM} , j_{s0} becomes

$$j_{s0} = \frac{\hbar}{2} \frac{(e-1)^2}{1+e^2} \frac{\lambda_{\text{HM}} \sigma_{\text{FM}}}{\lambda_{\text{HM}} \sigma_{\text{FM}} + \lambda_{\text{FM}} \sigma_{\text{HM}}} \frac{\theta_{\text{SH}} j_c}{q} \approx 0.35 \frac{\hbar}{2} \frac{\lambda_{\text{HM}} \sigma_{\text{FM}}}{\lambda_{\text{HM}} \sigma_{\text{FM}} + \lambda_{\text{FM}} \sigma_{\text{HM}}} \frac{\theta_{\text{SH}} j_c}{q}. \quad (22)$$

This j_{s0} is lesser than j_{s0} with the limits of $w_{\text{HM}} \gg \lambda_{\text{HM}}$ and $w_{\text{FM}} \gg \lambda_{\text{FM}}$.

We calculated numerically the spin current by using (12) to (19). The spin-diffusion lengths in the HM and FM were set to 1.0 nm and 2.0 nm, respectively. The following two types of the set $(w_{\text{HM}}, w_{\text{FM}})$ of the thicknesses of the HM and FM were chosen: $(w_{\text{HM}}, w_{\text{FM}}) = (15 \text{ nm}, 15 \text{ nm})$ and $(5.0 \text{ nm}, 1.0 \text{ nm})$. The situation of the thicknesses of $(15 \text{ nm}, 15 \text{ nm})$ was substituted for that of $w_{\text{HM}} \gg \lambda_{\text{HM}}$ and $w_{\text{FM}} \gg \lambda_{\text{FM}}$. The thicknesses of $(5.0 \text{ nm}, 1.0 \text{ nm})$ are often used for that of the HM/FM layer, namely, Ta/CoFeB and Pt/CoFeB layers, for the magnetization reversal with the spin-orbit torque.^{13),14)} Figure 2 shows the j_s normalized by $\hbar\theta_{\text{SH}}j_c/(2|q|)$, respectively. The j_s had positive values in the HM/FM layer in each situation. In other words, the spin current flowed to the $+z$ -direction in the HM owing to the SHE and flowed into the FM.

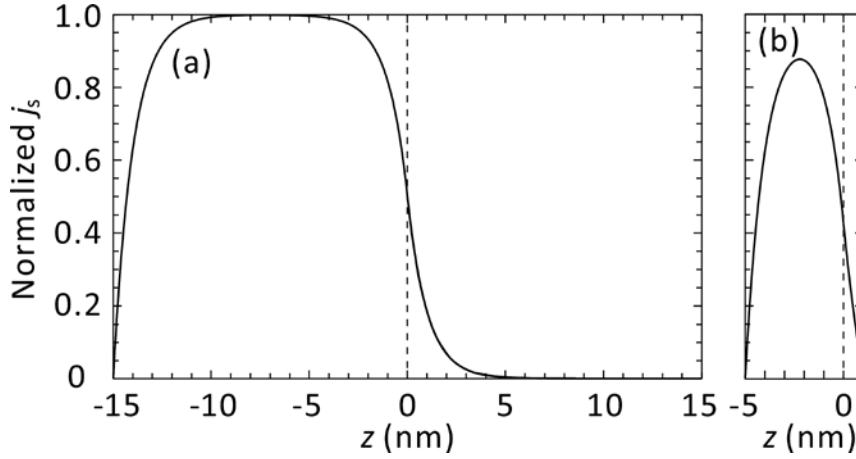


Fig. 2. Calculation results of the normalized spin current density in (a) 15-nm-HM/15-nm-FM layer and (b) 5-nm-HM/1-nm-FM layer.

When the thicknesses were $(w_{\text{HM}}, w_{\text{FM}}) = (15 \text{ nm}, 15 \text{ nm})$ (Fig. 2(a)), the spin current density was close to $\hbar\theta_{\text{SH}}j_c/(2|q|)$ inside the HM. This is because the spin was polarized sufficiently in the HM owing to the SHE. The spin current density decreased toward the interface. The spin current was more than zero at the interface and in the FM. This means that the spin current generated by the SHE flowed into the FM. The density of the spin current was $0.5\hbar\theta_{\text{SH}}j_c/(2|q|)$. The injected spin current decreased exponentially with increasing distance from the interface.

When the thicknesses were $(w_{\text{HM}}, w_{\text{FM}}) = (5.0 \text{ nm}, 1.0 \text{ nm})$ (Fig. 2(b)), the spin current density was lesser than $\hbar\theta_{\text{SH}}j_c/(2|q|)$ inside the HM. Since the HM thickness w_{HM} was not sufficiently long, the spin was not sufficiently polarized in the HM. The spin current density was approximately $0.43\hbar\theta_{\text{SH}}j_c/(2|q|)$ at the interface, which was lesser than that of the layer with $(w_{\text{HM}}, w_{\text{FM}}) = (15 \text{ nm}, 15 \text{ nm})$.

Figure 3 shows the differences of the spin-resolved electrochemical potentials including the SHE $\delta\mu$ in the HM/FM layer with $(w_{\text{HM}}, w_{\text{FM}})$ of (15 nm, 15 nm) and (5.0 nm, 1.0 nm). $\delta\mu$ was the maximum value at the HM surface in each HM/FM layer. Both $\delta\mu$ decreased monotonically with increasing z . This was consistent with the fact that the spin current flows to the $+z$ -direction in all regions in the HM/FM layer except $z = -w_{\text{HM}}$ and w_{FM} . In the region of $z > 5 \text{ nm}$ of the HM/FM layer with $(w_{\text{HM}}, w_{\text{FM}})$ of (15 nm, 15 nm), $\delta\mu$ was almost zero. Hence, the spin-up and down are equilibrium state. In other words, the spin diffused sufficiently in this region, and the spin current was zero in this region. In the HM/FM layer with $(w_{\text{HM}}, w_{\text{FM}})$ of (5 nm, 1 nm), $\delta\mu$ was larger than zero, even at the FM surface. This indicates that the spin did not diffuse sufficiently in the FM. This is one of the reasons why the spin current injected into the FM in the HM/FM layer with $(w_{\text{HM}}, w_{\text{FM}})$ of (5 nm, 1 nm) was lesser than that of the layer with $(w_{\text{HM}}, w_{\text{FM}}) = (15 \text{ nm}, 15 \text{ nm})$.

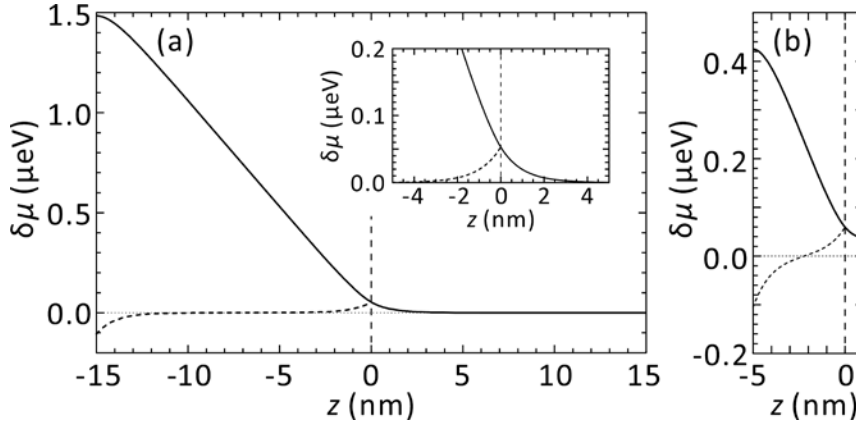


Fig. 3. Calculation results of the difference of the spin-resolved electrochemical potential including the SHE $\delta\mu$ in (a) 15-nm-HM/15-nm-FM layer and (b) 5-nm-HM/1-nm-FM layer. The solid curve indicates $\delta\mu$. The broken curve indicates the difference of the spin-resolved electrochemical potential without the SHE $\delta\mu'$. Inset of (a) shows an enlarged view of $\delta\mu$ around the interface of the HM/FM layer.

3 Discussion

We compare the above spin current with the spin current used in other studies. In the studies for the magnetization control owing to the spin-orbit torque, the density of the spin current injected into the FM is related to j_c and θ_{SH} as follows:^{4),15)}

$$j_{s0} = \frac{\hbar}{2} \frac{\theta_{SH} j_c}{q} \quad (23)$$

This is equal to the density of the spin current flowing near the center of the HM with $w_{HM} \gg \lambda_{HM}$. From (20) to (22), we find that the spin current injected into the FM is lesser than the spin current expressed by (23).

We have calculated the spin current using the electrochemical potential including the SHE. In other calculations of the spin current in the HM with the SHE, a spin-resolved electrochemical potential without the SHE (μ'_\uparrow and μ'_\downarrow) is usually used in the analysis of the spin current.¹⁶⁾ Examples of these potentials are given as

$$\mu'_\uparrow = eE_z + k_B T \frac{\delta n_\uparrow}{n_0}, \quad \mu'_\downarrow = eE_z + k_B T \frac{\delta n_\downarrow}{n_0}, \quad \delta\mu' = \mu'_\uparrow - \mu'_\downarrow = k_B T \frac{\delta n_\uparrow - \delta n_\downarrow}{n_0}, \quad (24)$$

where $\delta n_\uparrow = n_\uparrow - n_0$ and $\delta n_\downarrow = n_\downarrow - n_0$. Here, $n_{0\uparrow} = n_{0\downarrow} = n_0$ are assumed. Hence $j_\uparrow - j_\downarrow$ are given as

$$j_\uparrow - j_\downarrow = \frac{e}{\sigma} \frac{\partial \delta\mu'}{\partial z} + \theta_{SH} j_c. \quad (25)$$

All boundary conditions in this case are the same as the aforementioned boundary conditions. $\delta\mu'$ estimated with the same parameters with the aforementioned parameters are plotted by broken curves in Fig. 3. Since $\delta\mu'$ is proportional to $n_\uparrow - n_\downarrow$, $\delta\mu'$ corresponds to the spin accumulation. Hence, we can easily read the spin accumulation from the graph of $\delta\mu'$. Since

$\delta\mu'$ was maximum at the interface, we find that the spin most positively polarizes at the interface. Similarly, the spin most negatively polarized at the HM surface. Since the SHE does not occur in the FM, the values of $\delta\mu'$ are equal to those of $\delta\mu$ at the same z -positions in the FM. In the case of the HM/FM layer with 15-nm-width HM, the spin polarizability decreased exponentially with increasing distance from the interface in the FM and the density of spin-up n_{\uparrow} was similar to that of spin-down n_{\downarrow} at $z > 5$ nm. In the case of 1-nm-width HM, n_{\uparrow} is larger than n_{\downarrow} at $z = 1$ nm of the FM surface. When the SHE occurs, however, reading the spin current from the graph of $\delta\mu'$ may be difficult. Meanwhile, the gradient of $\delta\mu$ corresponds to the spin current. Hence we may easily read the spin current from the graph of $\delta\mu$. The gradient of $\delta\mu$ shown in Fig. 3 corresponds well to the spin current shown in Fig. 2.

When the density of spin-up is equal to the density of spin-down in the equilibrium state such as the HM, the difference between equation (1) and equation (2) becomes

$$\frac{d\delta n}{dt} = -\frac{1}{q} \frac{d\delta j}{dz} - \frac{\delta n}{\tau}, \quad (26)$$

where $\delta n = n_{\uparrow} - n_{\downarrow}$, $\delta j = j_{\uparrow} - j_{\downarrow}$, and $\tau_{\uparrow 0} = \tau_{\downarrow 0} = \tau$. Eq. (26) is often used as a continuity equation for the spin accumulation. Since τ is the spin relaxation time, which is the time required to return from the spin-accumulating state to the equilibrium state, the factor of τ is one in Eq. (26) and $\tau_{\uparrow 0}$ and $\tau_{\downarrow 0}$ are multiplied by two in the second and the third terms of Eqs. (1) and (2). When the density of spin-up is not equal to the density of spin-down in the equilibrium state such as FM, δn is defined as a difference from the density of spin in the equilibrium state.

4 Conclusion

We have calculated the spin current flowing through the HM/FM layer by using the spin-resolved electrochemical potential including the SHE $\delta\mu$. $\delta\mu$ has shown the current direction of the spin current. The spin current, which is generated in the HM owing to the SHE, has flown into the FM. For the FM with shorter spin diffusion length and larger conductivity, the amount of the spin current flowing into the FM has increased. When the thicknesses of the HM and the FM is similar to the spin-diffusion length or less, the amount of the spin current flowing into the FM decreases.

Acknowledgment

This work was supported by JSPS KAKENHI Grant Number JP20H02607, the Kansai University Fund for Supporting Outlay Research Centers 2020.

References

- 1) J. C. Slonczewski, Current-driven excitation of magnetic multilayers, *Journal of Magnetism and Magnetic Materials*, 159, L1-L7 (1996).
- 2) L. Berger, Emission of spin waves by a magnetic multilayer traversed by a current, *Physical*

- Review B*, **54**, 9353 (1996).
- 3) J. Katine, F. Albert, R. Buhrman, E. Myers, and D. Ralph, Current-driven magnetization reversal and spin-wave excitations in Co/Cu/Co pillars, *Physical Review Letters*, **84**, 3149 (2000).
 - 4) A. V. Khvalkovskiy, V. Cros, D. Apalkov, V. Nikitin, M. Krounbi, K. A. Zvezdin, A. Anane, J. Grollier, and A. Fert, Matching domain-wall configuration and spin-orbit torques for efficient domain-wall motion, *Physical Review B*, **87**, 020402(R) (2013).
 - 5) C. Song, R. Zhang, L. Liao, Y. Zhou, X. Zhou, R. Chen, Y. You, X. Chen, and F. Pan, Spin-orbit torques: Materials, mechanisms, performances, and potential applications, *Progress in Materials Science*, **118**, 100761 (2021).
 - 6) J. E. Hirsch, Spin Hall Effect, *Physical Review Letters*, **83**, 1834-1837 (1999).
 - 7) T. Jungwirth, J. Wunderlich, and K. Olejník, Spin Hall effect devices, *Nature Materials*, **11**, 382-390 (2012).
 - 8) S. Bhatti, R. Sbiaa, A. Hirohata, H. Ohno, S. Fukami, S. N. Piramanayagam, Spintronics based random access memory: a review, *materials today*, **20**, 530-548 (2017).
 - 9) S. S. P. Parkin, M. Hayashi, and L. Thoms, Magnetic domain-wall racetrack memory, *Science*, **320**, 190-194 (2008).
 - 10) A. Thiaville, Y. Nakatani, J. Miltat and Y. Suzuki, Micromagnetic understanding of current-driven domain wall motion in patterned nanowires, *Europhysics Letters*, **69**, 990 (2005).
 - 11) W. Zhang, V. Vlaminck, J. E. Pearson, R. Divan, S. D. Bader, and A. Hoffmann, Determination of the Pt spin diffusion length by spin-pumping and spin Hall effect, *Applied Physics Letters*, **103**, 242414 (2013).
 - 12) G. Zahnd, L. Vila, V. T. Pham, M. C.-Cheneau, W. Lim, A. Brenac, P. Laczkowski, A. Marty, and J. P. Attané, Spin diffusion length and polarization of ferromagnetic metals measured by the spin-absorption technique in lateral spin valves, *Physical Review B*, **98**, 174414 (2018).
 - 13) C. Zhang, S. Fukami, H. Sato, F. Matsukura, and H. Ohno, Spin-orbit torque induced magnetization switching in nano-scale Ta/CoFeB/MgO, *Applied Physics Letters*, **107**, 012401 (2015).
 - 14) Y. Chen, Q. Zhang, J. Jia, Y. Zheng, Y. Wang, X. Fan, and J. Cao, Tuning Slonczewski-like torque and Dzyaloshinskii-Moriya interaction by inserting a Pt spacer layer in Ta/CoFeB/MgO structures, *Applied Physics Letters*, **112**, 232402 (2018).
 - 15) L. S.-Tejerina, V. Puliafito, P. K. Amiri, M. Carpentieri, and G. Finocchio, Dynamics of domain-wall motion driven by spin-orbit torque in antiferromagnets, *Physical Review B*, **101**, 014433 (2020).
 - 16) S. Maekawa, S. O. Valenzuela, E. Saitoh, and T. Kimura, "Spin Current", Oxford: Oxford University Press, 2015.